



OPEN

A new method of accurate pedicle screw navigation

Daniel Suter^{1,2}✉, Aidana Massalimova¹, Christoph Johannes Laux², Laura Leoty¹, José Miguel Spirig², Florentin Liebmann¹, Fabio Carrillo¹, Philipp Fürnstahl¹ & Mazda Farshad²

One of the most established approaches to navigate pedicle screws is the planning and alignment (PA) method. Thereby a trajectory and associated entry point (EP) is planned and navigated after referencing to patient anatomy. However, deviations from the planned EP potentially lead to an altered screw position. The aim of this study was to investigate the influence of these EP deviations and to examine possible alternative methods. The merits of two new points of reference (screw tip point STP and midpoint MP) were therefore analyzed. STP represents the point on the optimal screw tip, MP the point at the center/midportion of the pedicle at its narrowest portion. The adapted screw trajectory was defined as the directional vector from any chosen EP to the STP or MP. First, computer simulations were used to evaluate the performance of these new approaches. Subsequently, the navigation technique yielding more acceptable screws in case of an EP deviation was analyzed on phantom-sawbone models. Both new methods showed a significantly larger number of possible screw trajectories in the simulations ($p < 0.01$). Even with a deliberate deviation of 4.5 mm (IQR 3.3) from the optimal EP, a perforation-free screw diameter of 4.9 mm (IQR 5.7 mm) could be achieved using the new navigation techniques. The simulated perforations were mainly located laterally with a median of 8.45 mm (IQR 3.95) distance to the medial pedicle wall. The PA method seems to be susceptible to EP deviations. The STP and MP methods are possible improvement mechanisms to overcome this disadvantage.

Keywords Pedicle screw navigation, Pedicle screw accuracy, Augmented reality, Computer assisted surgery, Spinal surgery.

Pedicle screw placement is a frequent intervention and misplacements are potentially harmful to neurovascular structures. Various pedicle screw navigation approaches have been investigated^{1–4} to reduce the reported rate of screw misplacements of between 1.2% and 41%^{5,6}. Currently, two main navigation approaches are used. Either a trajectory with an associated entry point (EP) is preoperatively planned and navigated after intraoperative referencing of the patient anatomy (planning and alignment (PA))^{1,7–9} or the position of a surgical tool and the patient anatomy is tracked and projected into imaging data (tool tracking (TT))^{10–14}. The advantage of the PA method is the possibility to carefully plan the geometrically optimal screw and to integrate preoperative offline data, such as bone mineral density or biomechanical calculations for screw placement¹⁵. In the PA method, the tool tip is typically first aligned to the EP and later to the trajectory. However, entry point deviations due to various reasons (e.g., hypertrophic facet joint, sclerotic bone, change of the vertebral surface after tissue removal, soft-tissue tension) frequently occur and potentially render the navigation with the PA method useless.

The aim of this study was to investigate the influence of an EP deviation in the PA method and to examine possible alternative methods allowing for intraoperative adaptation of the screw trajectory. As such, we investigated the merits of the screw tip point (STP) and the pedicle midpoint (MP) over the EP as reference points. The MP thereby represents the center point of the pedicle at its narrowest diameter, the STP the tip of the optimal pedicle screw.

Methods

We hypothesized that accounting for EP deviations the two new mechanisms outperforms the current PA method regarding the amount of clinically acceptable pedicle screws (< 2 mm perforation).

¹Research in Orthopedic Computer Science, University Hospital Balgrist, University of Zurich, Forchstrasse 340, Zurich 8008, Switzerland. ²Spine Division, Department of Orthopedic Surgery, Balgrist University Hospital, University of Zurich, Forchstrasse 340, Zurich 8008, Switzerland. ✉email: dapesu@bluewin.ch

To test the hypothesis we compared the methods in a computer simulation and tested the results with real pedicle screw placements on a lumbosacral spine training phantom (L1 to coccyx and pelvis, Synbone AG, Zizers, Switzerland).

Planning and update mechanisms

For the computer simulations 3D vertebral body models of the five lumbar vertebrae (L1–L5) of a spinal statistical shape model (29) were utilized. In the second series of experiments, 3D models of the aforementioned phantom were used. These 3D models were uploaded to the surgery planning software CASPA (CASPA, version 5.26, Balgrist, Zurich, Switzerland). The planning of each pedicle screw and its associated parameters was carried out as follows:

- A 3D plane was created and placed through the thinnest portion of each pedicle (see Fig. 1). The plane was manually aligned in the axial plane to the thinnest pedicle portion. Then, the optimal antero-posterior angulation was adjusted in the sagittal view.
- Based on the CASPA functionality called “intersection”, a cross-sectional cut between plane and pedicle was calculated to obtain the projected 2D pedicle outline at its smallest diameter. The center of this outline defined the MP.
- A trajectory was placed through the MP, which was later visually aligned to the corresponding pedicle axis in the axial view and chosen to be parallel to the upper vertebral endplate in the sagittal view.
- To define the STP, four planes parallel to the coronal plane were inserted, separating the vertebral body into five equal parts. The STP was then defined as a point on the pedicle trajectory at the transition from the fourth to the fifth fifth of the vertebral body (see Fig. 1).
- The optimal EP was finally defined as the intersection between the optimal trajectory and the dorsal surface of the vertebral body.
- The screw diameter was set to fill the pedicle at its smallest diameter.

This planning process provides the definitions of the MP and STP. The reason to use the two is based on their localization. As the center of the pedicle at its narrowest point dictates the maximum possible screw diameter it may serve as an appropriate reference for an updated trajectory. If matched exactly, the thickest perforation free screw can be set. However, the theoretical danger is that small deviations in the EP may lead to strong deviations in the trajectory, since the MP is close to the EP. Therefore, we compared the MP to a reference point more anterior and thus more robust to EP deviation. As such, we defined the STP which represents the tip of the optimal pedicle screw.

The following update mechanism were evaluated for intraoperative deviations from the optimal EP:

- Let A be the planned EP to any given vertebra. The corresponding optimal trajectory is represented as the vector from the EP A to a point B on the optimal trajectory ($= \overrightarrow{AB}$). Let C then be any deviated EP (EP_dev) on the vertebra surface. The corresponding deviated trajectory shall be the vector from the EP_dev to a point D on the same deviated trajectory ($= \overrightarrow{CD}$). The MP shall be a point E and the STP shall be a point F.
- Execution without Update: The planned optimal trajectory \overrightarrow{AB} through the optimal EP is shifted in parallel to EP_dev ($\overrightarrow{AB} = \overrightarrow{CD}$).
- Adaption to MP reference point: The updated trajectory is defined as vector from C to MP (\overrightarrow{CE}).
- Adaption to STP reference point: The updated trajectory is defined as vector from C to STP (\overrightarrow{CF}).

Computer-based evaluation

To compare the STP and MP update mechanisms to the execution without update, we performed a computer simulation in MATLAB (MATLAB, version 7.10.0 (R2010a), Natick, Massachusetts: The MathWorks Inc.). Following the described planning (see “Planning and update mechanisms”) the defined parameters (3D models, MP, STP, optimal screw trajectory and optimal EP) were uploaded into MATLAB. Additionally to the aforementioned planning, a coordinate system for each vertebra and the area in which EP deviations may occur ($= \text{areaEP}$) (see Fig. 2) were defined. The origin of the coordinate system was set at the center of the spinal canal (see Fig. 2). AreaEP was created by an experienced spine surgeon by manually marking the region on the vertebral body mesh around the optimal EP that represents clinically observable deviations in 3-matic (3-matic, Materialise NV, Leuven, Belgium). Trajectories for the different EP_dev were calculated using the STP and MP methods (see section “Planning and update mechanisms”). Simulated EP_dev were obtained by sampling areaEP with an accuracy of one point per square mm.

The first two simulations were based on the STP and MP method. The third simulation was intended to evaluate the effect of an EP deviation without update mechanism. For this purpose, a trajectory parallel to the optimal trajectory was simulated by each EP_dev.

Consecutively, cylinders representing different screw diameters (5–7.5 mm in 0.5 mm steps) were assigned to each of the calculated trajectories. The function `in_polyhedron`¹⁶ was then used to determine whether the points of the pedicle wall were inside or outside of the cylinder mesh. If a pedicle point was inside the cylinder ($= \text{perforation}$), the shortest distance between pedicle point and cylinder was reported as perforation depth. The subset of pedicle screw trajectories with acceptable breach (Gertzbein–Robbins grades A and B¹⁷) were recorded for each method (STP, MP, and PA method) and each cylinder diameter (5–7.5 mm). This subset was noted as a percentage of all possible EP_dev of areaEP and thus represented a direct performance indicator of the method’s adaptability.

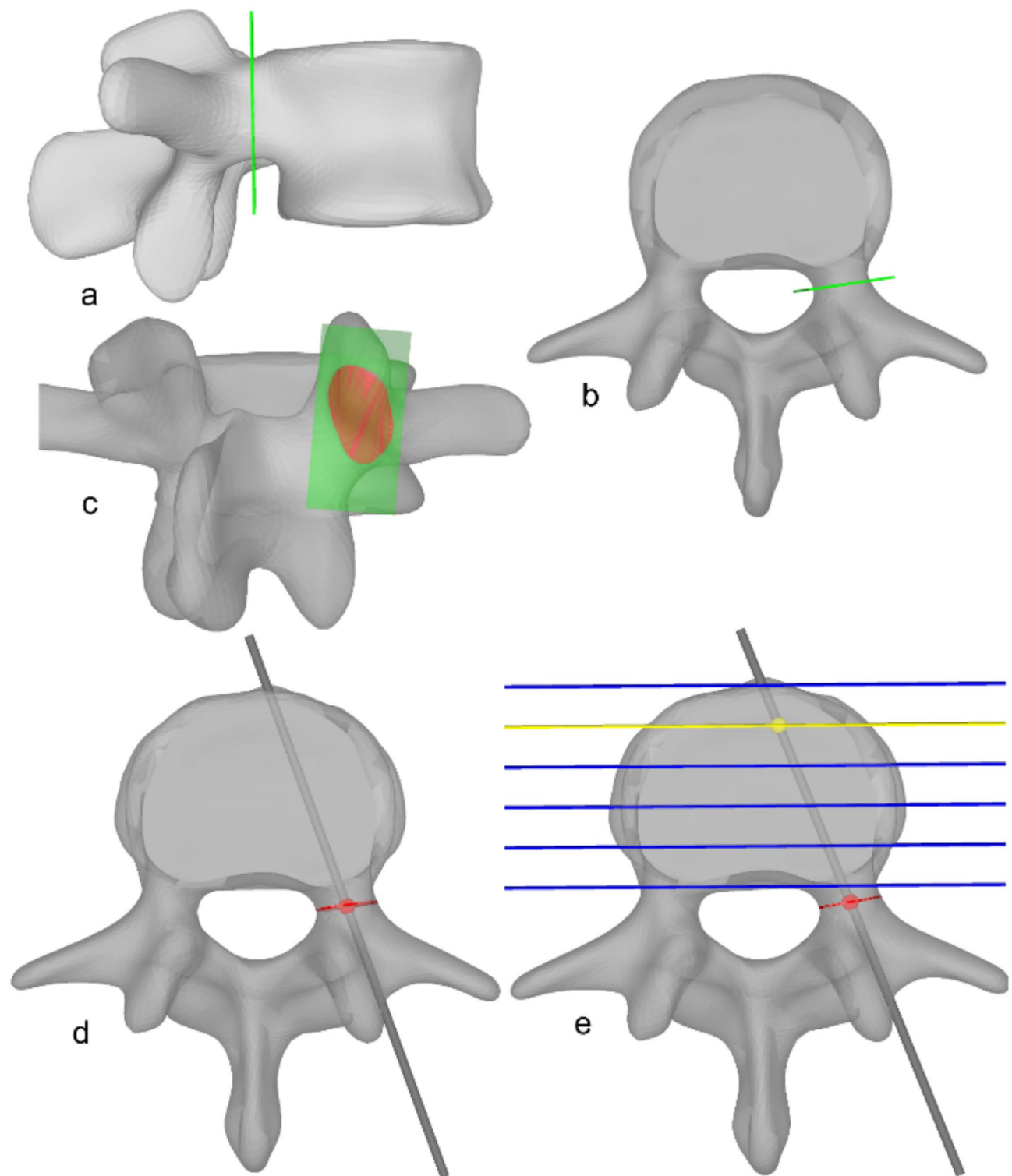


Fig. 1. Planning description showing the process on an axial view on the 3D model from generating the plane through the thinnest portion (b), placing OT through the MP (d) and defining STP (e). Additionally 3D model with the generated plane through the thinnest portion in sagittal (a), axial (b) and posterior (c) view. Plane through thinnest pedicle portion = green area; projected 2D pedicle outline = red area; MP = red point; OT = grey line; cutting plane between each fifth of vertebra = blue line; transition fourth fifth to fifth fifth = yellow line; STP = yellow point. Original image generated using CASPA (CASPA, version 5.26, Balgrist, Zurich, Switzerland). Image compilation and editing with paint.net (Paint.NET, Version 5.1.2, DotPDN LLC, Seattle, United States, <https://www.getpaint.net/>).

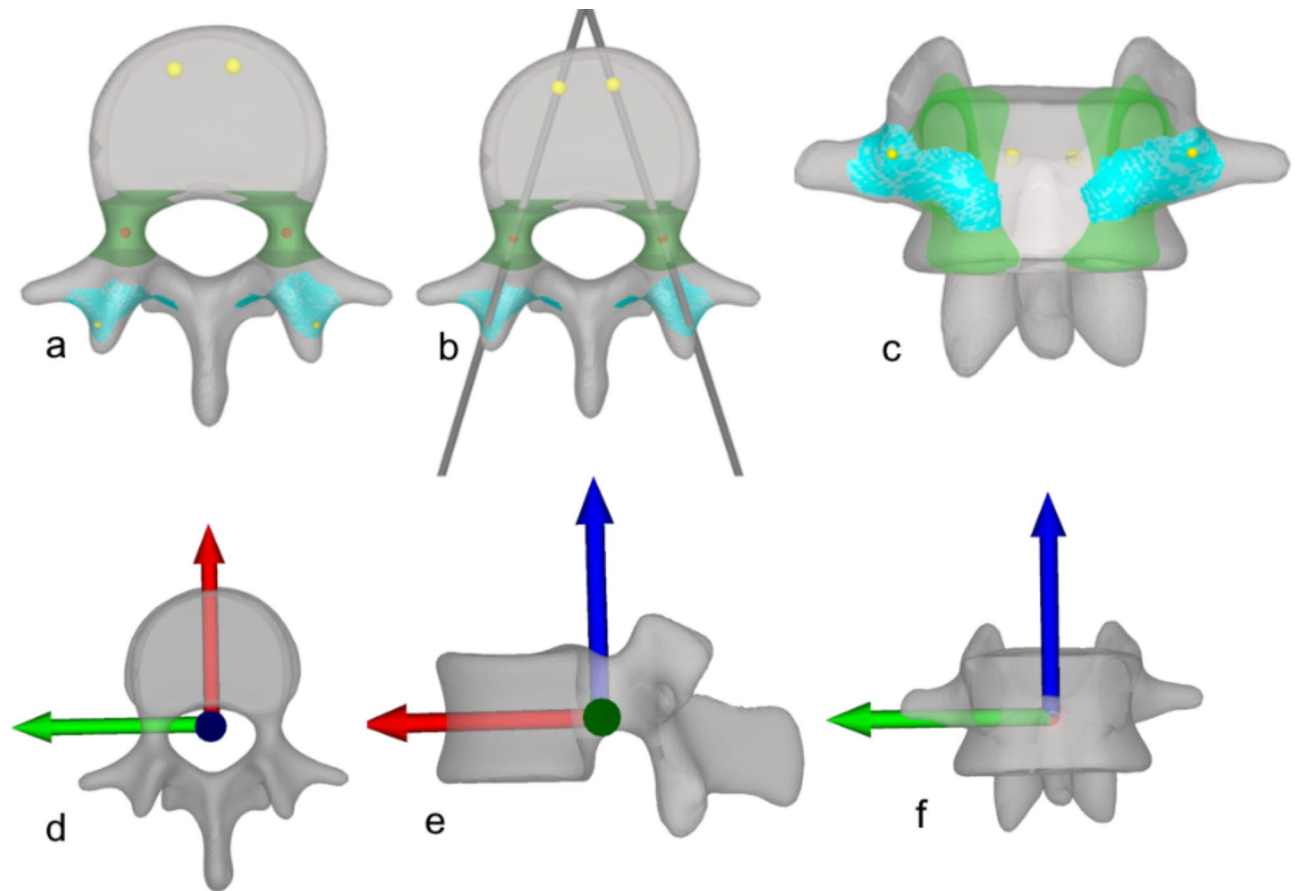


Fig. 2. Fully prepared 3D vertebra model in axial view without OT (a) axial view with OT (b) and posterior view (c) as well as 3D model with coordinate system in all 3 views (d=axial, e=sagittal and f = posterior); STP = big yellow point; MP = red point; EP = small yellow point; OT = grey line; areaEP = blue area; pedicle mesh = green area. Original image generated using CASPA (CASPA, version 5.26, Balgrist, Zurich, Switzerland). Image compilation and editing with paint.net (Paint.NET, Version 5.1.2, DotPDN LLC, Seattle, United States, <https://www.getpaint.net/>).

Phantom-based evaluation

To confirm the simulation results and to invest its adaptability real pedicle screw trajectories were drilled in the Synbone phantom using the best-performing update mechanism (STP). Optical navigation based on fusion Track 500 system (Atracsys LLC, Puidoux, CH) was employed to guide screw placement. The phantom and a commercial drill sleeve (\varnothing 3.2 mm No. 03.614.010, Synapse System, DePuy Synthes, Johnson & Johnson, Raynham, MA, USA, see Fig. 3) were tracked via custom-designed markers consisting of four infrared spheres (see Fig. 3). Preoperative planning was performed according to section “Planning and update mechanisms”. The optimal trajectory and the corresponding EP were represented by a green line and point. Additionally, the corresponding 3D model of the vertebral body was displayed. A red line represented the current trajectory of the tracked drill sleeve (see Fig. 3).

Six surgeons (one resident, five experienced spine surgeons) performed the experiments. All the experience surgeon are bord certified orthopedic surgeons with at least 3 years' experience in spinal surgery. All study participants (including the resident) have been investigators in many other studies conducting navigation in spinal surgery. Each surgeon drilled five pedicle screw trajectories using the STP method without deviation. In addition, each surgeon drilled ten pedicle screw trajectories using the STP method with deviation from the optimal EP. The surgeons where instructed to create clinically realistic deviations, but amount and direction were decided on an ad-hoc basis. To facilitate segmentation and 3D reconstruction of the drilled screw trajectories, radiolucent graphite leads were inserted into the drilled pedicles.

After CT acquisition (SOMATOM Edge Plus, Siemens Healthcare GmbH, Erlangen, Germany, slice thickness: 0.75 mm, in-plane resolution: 0.5×0.5 mm), the scans of the phantoms were segmented using Mimics (Mimics Medical software, version 19.0; Materialize NV, Leuven, Belgium) and imported in CASPA for 3D analysis.

Measured outcome parameters were the Euclidean distance between planned and performed STP (STP difference), the 3D angle between the navigated and performed trajectory (direction difference) as well as the maximum screw diameter without perforation and the maximum screw diameter to medial breach. The postoperatively segmented vertebrae were registered to the corresponding 3D models of the planning. STP

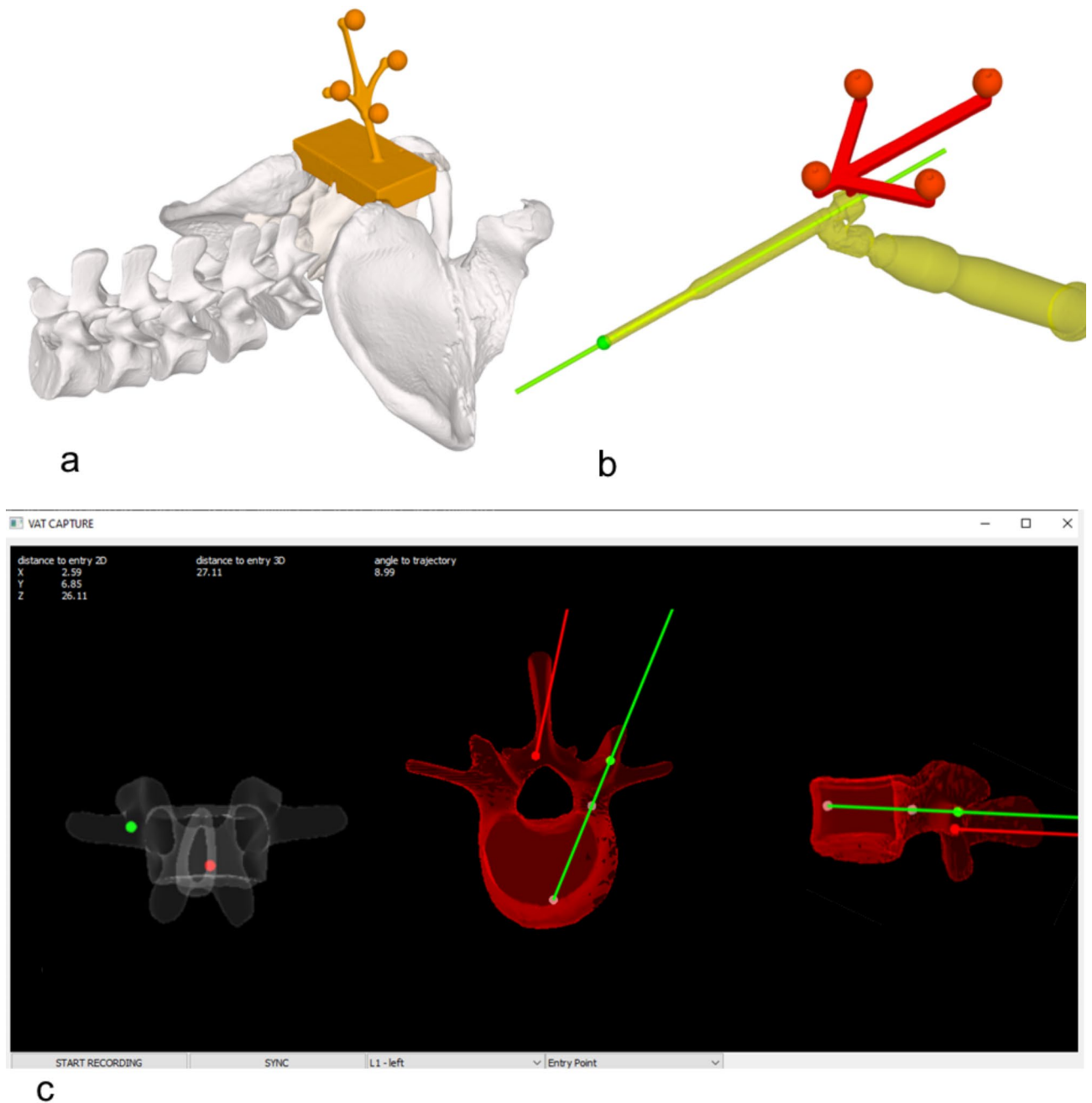


Fig. 3. (a) 3D model of lumbosacral spine training phantom and (b) drill sleeve equipped with infrared spheres as well as (c) visualization of PA method in navigation program. Image generated during Navigation using an in house developed program based on python (Python Software Foundation. Python Language Reference, version 3.9.5. Available at <http://www.python.org>).

difference was calculated as the orthogonal distance between the planned and performed screw trajectories at the level of the preoperative STP (see Fig. 4). Consecutively, the direction difference for the used EP as well as the maximum screw diameter without perforation and the maximum screw diameter to medial breach were calculated. Additionally, the Euclidean distance from EP_dev to the planned EP (DEV) was calculated as measurement for the deviation during these trials.

Statistics

Descriptive statistics were reported as median and IQR for skewed data and as counts and percentage for categorical variables. Normal distribution was assessed by plotting the data. Differences between the amounts of acceptable simulated screws per method (STP, MP, and PA method) were evaluated using Kruskal Wallis test. Differences regarding STP difference, direction difference, maximum screw diameter without perforation, and

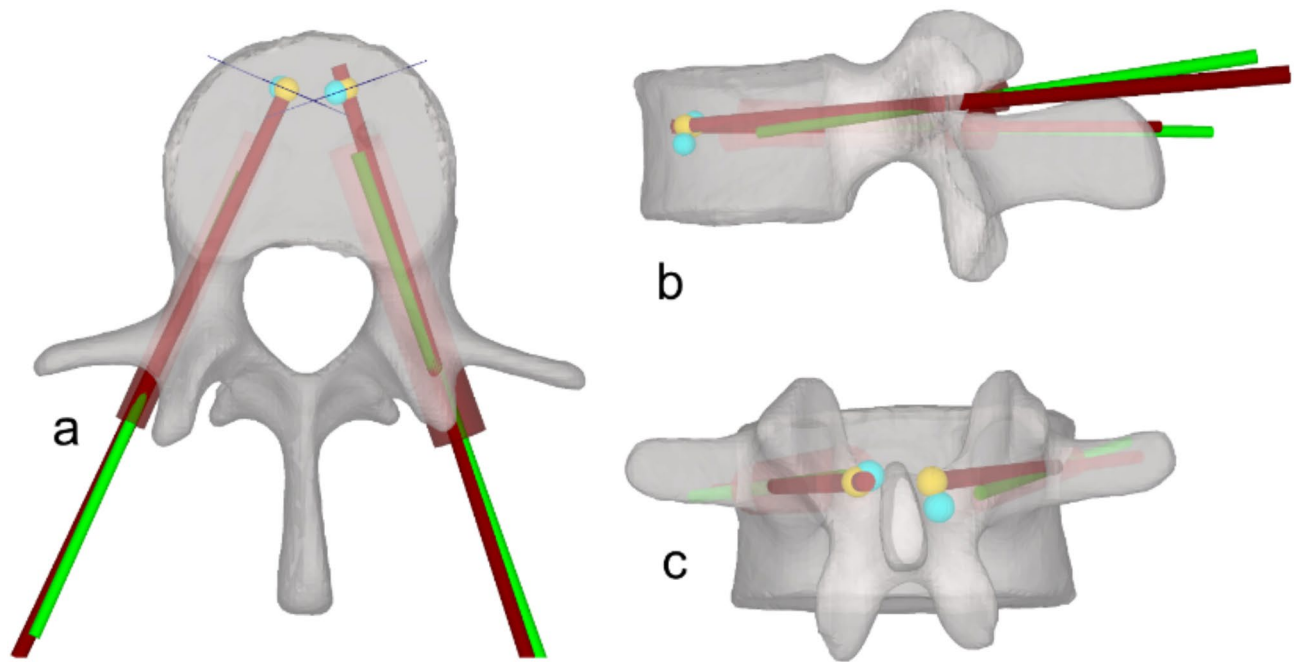


Fig. 4. Preoperative and postoperative vertebra registered to each other with their corresponding screw trajectories and STP's in (a) axial, (b) sagittal and (c) posterior view; registered cylinder to graphite mine = green line; calculated planned trajectory = red line; planned STP = yellow point; performed STP = blue point; estimated perforation-free screws = transparent big red cylinder; orthogonal plane to red line through planned STP = thin blue line. Original image generated using CASPA (CASPA, version 5.26, Balgrist, Zurich, Switzerland). Image compilation and editing with paint.net (Paint.NET, Version 5.1.2, DotPDN LLC, Seattle, United States, <https://www.getpaint.net/>).

the maximum screw diameter to medial breach were assessed using t-test. The significance was set <0.05 . Data were analyzed with Phyton (Version 3.9.5.).

A post-hoc power analysis was conducted using chi-square to determine whether the sample size was sufficient to detect differences between the three methods regarding screw perforation rates.

Results

Computer-based evaluation

For both the STP and the MP method, a greater amount of EP_dev within areaEP resulted in valid screw trajectories compared to the PA method (see Fig. 5; Tables 1, 2 and 3). More screws with acceptable breach could be simulated with the STP method than with the MP method (see Fig. 5; Table 4). In comparison to the MP and PA methods, the STP method showed additional possible EP_dev in the lateral region (see Figs. 6 and 7). The post-hoc power analysis yielded a power of 1 for both the percentage of screws without perforation ($w=0.472$, $N=46,130$, $df=2$, $\alpha=0.05$) and the percentage of screws with acceptable perforation ($w=0.175$, $N=84,294$, $df=2$, $\alpha=0.05$), indicating a sufficient sample size.

Phantom-based evaluation

A median maximum screw diameter without perforation of 8.8 mm (IQR 5.1 mm) and median maximum screw diameter to medial breach of 7.6 mm (IQR 4.05 mm) were found. The median for the STP difference was 4.45 mm (IQR 2.54 mm). The median direction difference was 5.18° (IQR 2.9°).

For EP deviations, a maximum screw diameter without perforation of 4.9 mm (IQR 5.7 mm) was found with a median DEV of 4.5 mm (IQR 3.3 mm). In 84% of the trials the deviation was lateral and in 68% cranial to the planned EP. In 42% DEV was >5 mm and in 16% >8 mm. In 26% DEV was <3 mm. The median maximum screw diameter without perforation for trials with a DEV >5 mm was 3.2 mm (IQR 3 mm). In the trials with DEV <5 mm, the median maximum screw diameter without perforation was 6.6 mm (IQR 3.8 mm).

Discussion

Our simulations showed that with both the MP and the STP method a significantly larger number of clinically acceptable screws can be placed compared to the PA method. In the PA method, only small EP deviations are tolerable. The deviation from the planned EP therefore plays a decisive role in the PA method and causes potential harm to neurovascular structures. When comparing the STP and MP methods, more screws with clinically acceptable perforation could be computed using the STP method.

In the plot of possible EP_dev on the areaEP for both methods, it is noticeable that more medial EP's are feasible using the MP method. Laterally, the STP method offers more acceptable EP's. The elevated danger of

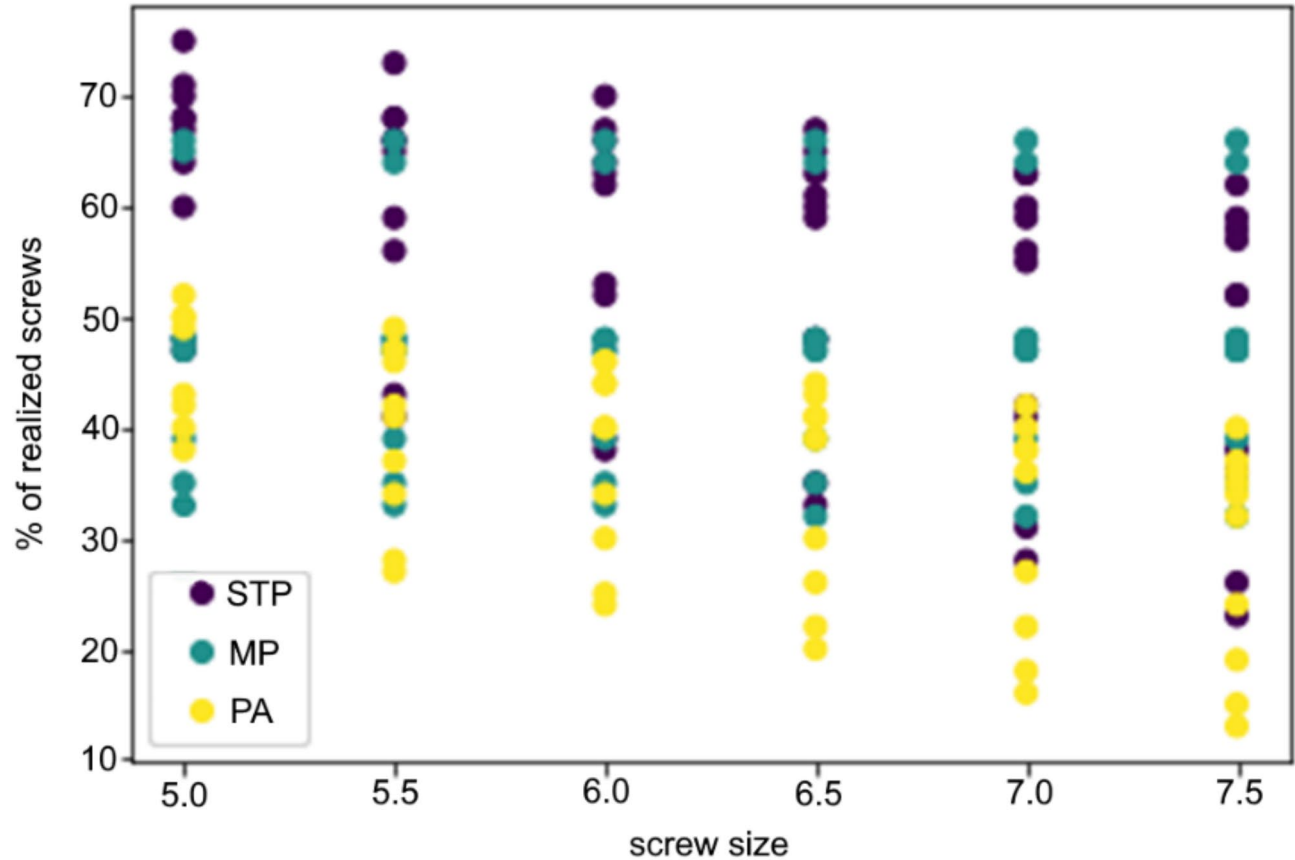


Fig. 5. Plot of screw size to EP_dev with acceptable perforation (Gertzbein-Robbins grade B, < 2 mm).

Screw diameter	STP method	MP method	PA method	p-value
5 mm	67% (IQR 9%)	48% (IQR 7%)	42% (IQR 11%)	<0.01
5.5 mm	65% (IQR 11%)	48% (IQR 7%)	41% (IQR 12%)	<0.01
6 mm	62% (IQR 13%)	47% (IQR 7%)	40% (IQR 13%)	<0.01
6.5 mm	59% (IQR 15%)	47% (IQR 7%)	39% (IQR 14%)	<0.01
7 mm	55% (IQR 19%)	47% (IQR 7%)	37% (IQR 14%)	<0.01
7.5 mm	52% (IQR 21%)	47% (IQR 7%)	33% (IQR 16%)	<0.01

Table 1. Percentage of all possible EP_dev of areaEP for each method (STP, MP and PA method) and screw diameter with accepted perforation. P-values calculated with Kruskal Wallis test; significant values marked bold. Highest % are highlighted in italics.

Screw diameter	STP method	PA method	p-value
5 mm	67% (IQR 9%)	42% (IQR 11%)	<0.01
5.5 mm	65% (IQR 11%)	41% (IQR 12%)	0.04
6 mm	62% (IQR 13%)	40% (IQR 13%)	<0.01
6.5 mm	59% (IQR 15%)	39% (IQR 14%)	<0.01
7 mm	55% (IQR 19%)	37% (IQR 14%)	<0.01
7.5 mm	52% (IQR 21%)	33% (IQR 16%)	<0.01

Table 2. Percentage of all possible EP_dev of areaEP for STP and PA method as well as screw diameter with accepted perforation. P-values calculated using t-test; significant values marked bold. Higher % are highlighted in italics.

Screw diameter	MP method	PA method	<i>p</i> -value
5 mm	48% (<i>IQR 7%</i>)	42% (<i>IQR 11%</i>)	0.25
5.5 mm	48% (<i>IQR 7%</i>)	41% (<i>IQR 12%</i>)	< 0.01
6 mm	47% (<i>IQR 7%</i>)	40% (<i>IQR 13%</i>)	0.03
6.5 mm	47% (<i>IQR 7%</i>)	39% (<i>IQR 14%</i>)	0.01
7 mm	47% (<i>IQR 7%</i>)	37% (<i>IQR 14%</i>)	< 0.01
7.5 mm	47% (<i>IQR 7%</i>)	33% (<i>IQR 16%</i>)	< 0.01

Table 3. Percentage of all possible EP_dev of areaEP for MP and PA method as well as screw diameter without and accepted perforation. P-values calculated using t-test; significant values marked bold. Higher % are highlighted in italics.

Screw diameter	STP method	MP method	<i>p</i> -value
5 mm	67% (<i>IQR 9%</i>)	48% (<i>IQR 7%</i>)	< 0.01
5.5 mm	65% (<i>IQR 11%</i>)	48% (<i>IQR 7%</i>)	0.03
6 mm	62% (<i>IQR 13%</i>)	47% (<i>IQR 7%</i>)	0.06
6.5 mm	59% (<i>IQR 15%</i>)	47% (<i>IQR 7%</i>)	0.23
7 mm	55% (<i>IQR 19%</i>)	47% (<i>IQR 7%</i>)	0.65
7.5 mm	52% (<i>IQR 21%</i>)	47% (<i>IQR 7%</i>)	0.86

Table 4. Percentage of all possible EP_dev of areaEP for STP method and MP method as well as screw diameter with accepted perforation. P-values calculated using t-test; significant values marked bold. Higher % are highlighted in italics.

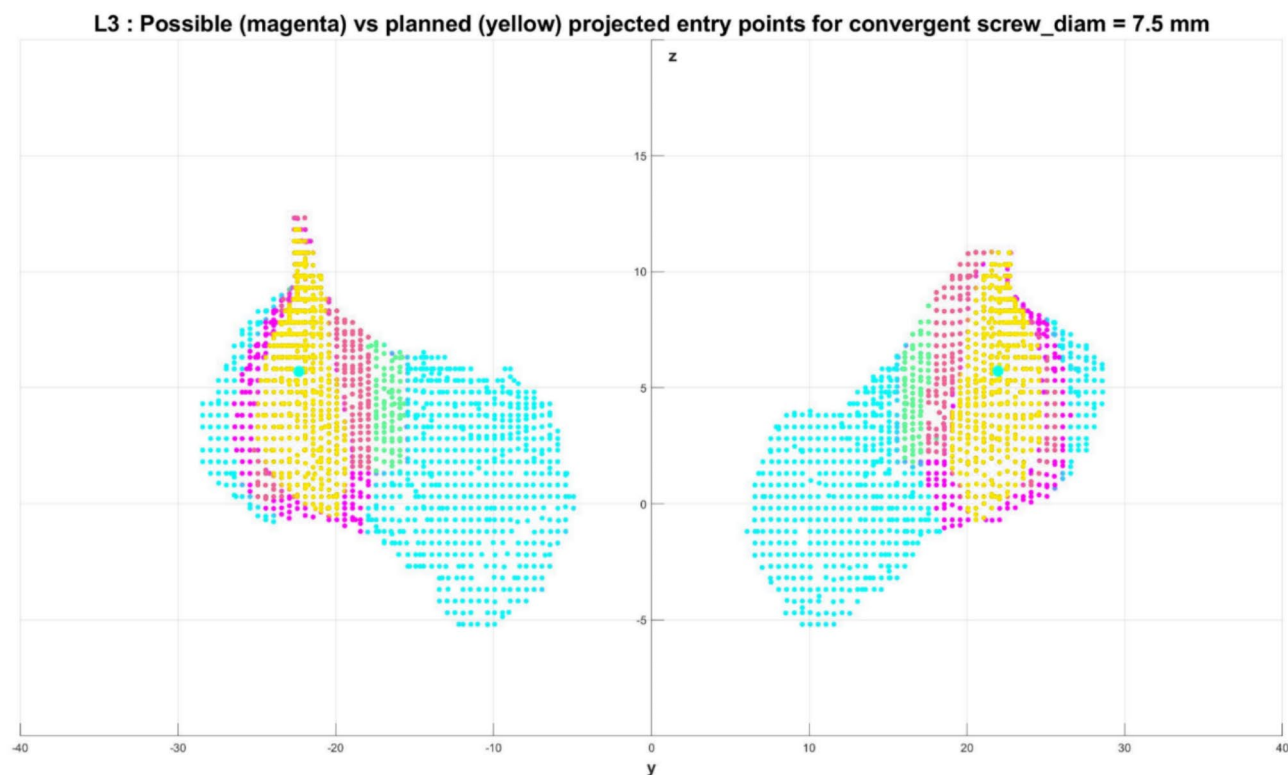


Fig. 6. Plot of possible EP_dev for each method (STP, MP and PA method) on areaEP from the used L3 model; optimal EP = big blue point; unused EP_dev from areaEP = small blue points; from all 3 method used EP_dev = yellow points; only via STP method used EP_dev = magenta; only via MP method used EP_dev = green points; via STP and MP method used EP_dev = brown points. Image generated using MATLAB (MATLAB. version 7.10.0 (R2010a). Natick, Massachusetts: The MathWorks Inc.).

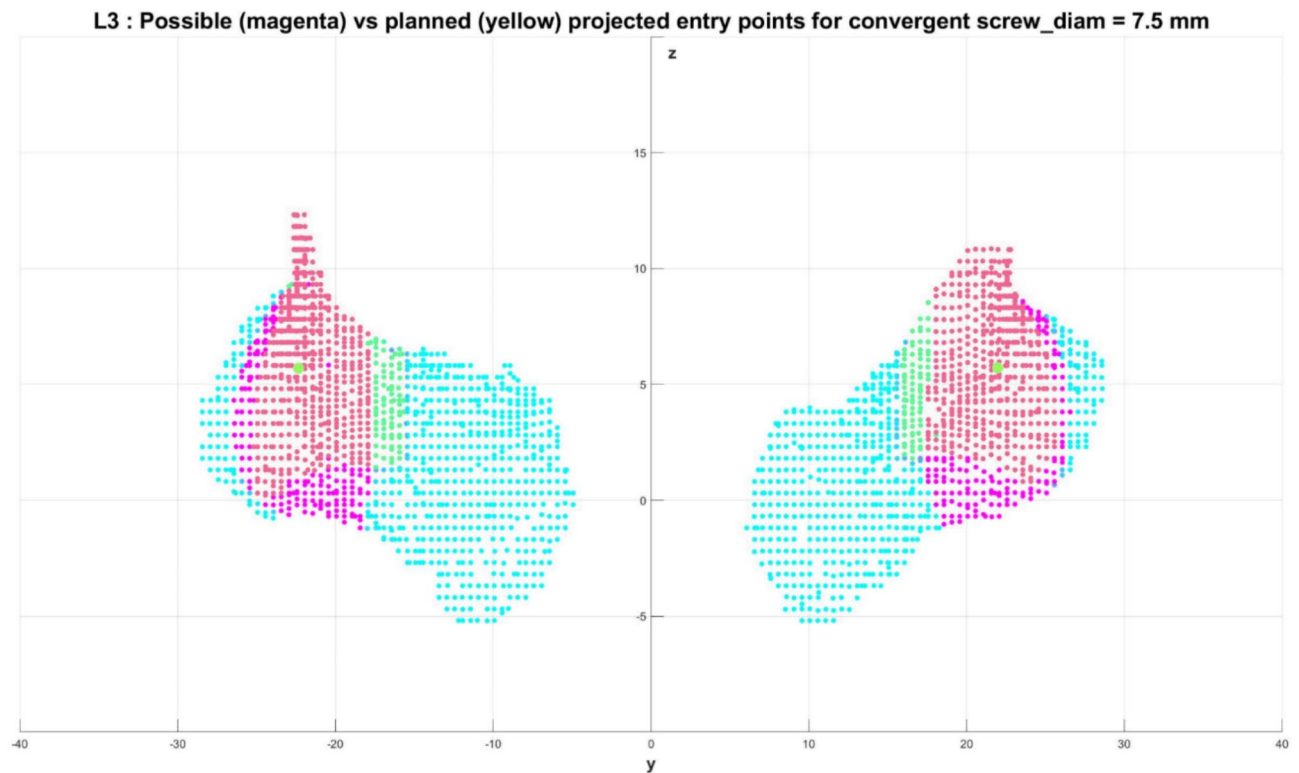


Fig. 7. Plot of possible EP_{dev} for STP method and MP method on areaEP from the used L3 model; optimal EP = big green point; unused EP_{dev} from areaEP = small blue points; only via STP method used EP_{dev} = magenta point; only via MP method used EP_{dev} = green points; via STP and MP method used EP_{dev} = brown points = brown points. Image generated using MATLAB (MATLAB, version 7.10.0 (R2010a). Natick, Massachusetts: The MathWorks Inc.).

a medial breach, the more extreme convergence or divergence angles, the lower number of realizable pedicle screws, the clinically less favorable distribution of feasible EP's with the MP method led to our decision to focus on the STP method. However, both update methods give the surgeon more possibilities to choose an EP in comparison to the PA method.

With a median deviation of 4.5 mm, a perforation-free screw diameter of 4.9 mm (IQR 5.7 mm) could still be achieved in case of a deviation from the optimal EP using the STP method. Intraoperative adaptation of the planned trajectory using the STP method is hence feasible. With a median maximum screw diameter to medial breach of 8.45 mm (IQR 3.95 mm), the deviated screws were also found to perforate laterally. This is well in line with the lateral extension of the areaEP field in the simulations. Studies indicate that lateral perforations are better tolerated clinically⁶ and safe zones of <6 mm for lateral perforation are reported in the literature^{18,19}. Therefore the STP method therefore allows for safer screws regarding the neurovascular structures.

Due to the more lateral deviation, the STP method allows for screw positioning without damaging the facet joints. Even though the reduction of a hypertrophic facet is a valid method to define the entry point, this might be unfavorable with regards to the upper instrumented vertebra since a violation of the superior facet (or even the facet joint capsule) has been shown to be a major risk factor for adjacent segmental degeneration^{20,21}.

However, lateral screws could be disadvantageous with regard to the stability of the construct. Lateral perforations were shown to reduce pull-out strength by 30%, whereas medial perforations actually increased pull-out strength^{22,23}. Thus, a too far lateral deviation needs to be avoided with the STP method.

The accuracy of the navigation in terms of STP difference with 4.45 mm (IQR 2.54 mm) was at the lower end when compared to the literature^{10,24,25}. Reported mean deviations from the planned entry point range from 1.4 mm \pm 0.8 mm to 4 mm \pm 2.7 mm in literature. However, to our knowledge, this is the first study to navigate the STP. The studies mentioned above each navigated the EP, which is why a direct comparison based on the deviation from the planned point is difficult.

Limitations

The simulation was only carried out on an average shape model calculated from a representative population. However, our data are the first of their kind and therefore may provide an important basis for initiating further studies. It remains to be investigated how well the methods work on real human anatomy. The next step in this regard would be experiments on human cadavers.

Selection bias may have occurred during the phantom-based experiments, specifically in the testing of the STP method without deviation, since the only randomization was if the surgeon started with L1 left or right.

Parameter	Comparison	Kruskal-Wallis <i>p</i> -value	Post-hoc <i>p</i> -values
Screw tip difference	L1 vs. L2	–	1
	L1 vs. L3		0.89
	L1 vs. L4		1
	L1 vs. L5		0.89
	L2 vs. L3		0.89
	L2 vs. L4		1
	L2 vs. L5		0.89
	L3 vs. L4		0.89
	L3 vs. L5		0.89
	L4 vs. L5		1
	left vs. right	–	0.48
Maximum screw diameter without perforation	L1 vs. L2	0.0045	0.6276
	L1 vs. L3		0.0581
	L1 vs. L4		0.0071
	L1 vs. L5		0.0058
	L2 vs. L3		0.0581
	L2 vs. L4		0.0071
	L2 vs. L5		0.0175
	L3 vs. L4		0.0581
	L3 vs. L5		0.0589
	L4 vs. L5		0.7478
	left vs. right	–	0.79
Maximum screw diameter to medial breach	L1 vs. L2	0.0216	0.492
	L1 vs. L3		1
	L1 vs. L4		0.32
	L1 vs. L5		0.024
	L2 vs. L3		0.422
	L2 vs. L4		0.076
	L2 vs. L5		0.02
	L3 vs. L4		0.183
	L3 vs. L5		0.02
	L4 vs. L5		0.044
	left vs. right	–	0.14

Table 5. Difference in-between levels and sides in regard to the three measured parameters in the Phantom based evaluation. P-values calculated Kruskal-Wallis and Wilcoxon-test; significant values marked bold.

For the following levels for each surgeon, the side was alternated (for example L1 left, L2 right, L3 left, L4 right, L5 left). To test the effect of the bias, we conducted a Kruskal-Wallis- and post-hoc Wilcoxon-test (see Table 5). On this basis, we could not identify any significant difference between left and right side. The differences found concerned the parameters maximum screw diameter without perforation and maximum screw diameter to medial breach, particularly between upper vertebral levels to lower. However, this could also be explained mainly by the difference in pedicle diameter. The second half of the phantom-based evaluation was completely randomized and therefore not at risk of a selection bias.

Conclusion

EP deviations pose a relevant problem when performing pedicle screw placement using the PA method. The STP method seems to be a feasible alternative to the established, less flexible PA method. The main advantage of the STP method is the possible adaptation of the screw trajectory to real intraoperative conditions, which makes it the first adjustable navigation method. Perforations were found to occur more laterally than medially with the STP method. Injury to neurovascular structures is thus less likely even in the case of pedicle perforation. However, in order to be able to make generalizable statements and test the feasibility in clinical practice, further studies on cadavers and ultimately in patients are required.

Data availability

The datasets generated during and/or analysed during the current study are available from the corresponding author on reasonable request.

Received: 7 October 2024; Accepted: 24 February 2025

Published online: 12 March 2025

References

- Liebmann, F. et al. Pedicle screw navigation using surface digitization on the Microsoft hololens. *Int. J. Comput. Assist. Radiol. Surg.* **14**(7), 1157–1165. <https://doi.org/10.1007/s11548-019-01973-7> (2019).
- Laudato, P. A., Pierzchala, K. & Schizas, C. Pedicle screw insertion accuracy using O-Arm, robotic guidance, or freehand technique: a comparative study. *Spine (Phila Pa. 1976)* **43**(6), E373–E378. <https://doi.org/10.1097/brs.0000000000002449> (2018).
- Shin, B. J., Njoku, J. A. R. & Härtl, I. U. Pedicle screw navigation: a systematic review and meta-analysis of perforation risk for computer-navigated versus freehand insertion. *J. Neurosurg. Spine* **17**(2), 113–122. <https://doi.org/10.3171/2012.5.spine11399> (2021).
- Mason, A. et al. The accuracy of pedicle screw placement using intraoperative image guidance systems. *J. Neurosurg. Spine* **20**(2), 196–203. <https://doi.org/10.3171/2013.11.SPINE13413> (2014).
- Amato, V., Giannachi, L., Irace, C. & Corona, C. Accuracy of pedicle screw placement in the lumbosacral spine using conventional technique: computed tomography postoperative assessment in 102 consecutive patients. *J. Neurosurg. Spine* **12**(3), 306–313. <https://doi.org/10.3171/2009.9.spine09261> (2010).
- Saarenpää, I. et al. Accuracy of 837 pedicle screw positions in degenerative lumbar spine with conventional open surgery evaluated by computed tomography. *Acta Neurochir. (Wien.)* **159**(10), 2011–2017. <https://doi.org/10.1007/s00701-017-3289-7> (2017).
- Farshad, M. et al. Direct augmented reality navigated pedicle screw placement and rod bending. *N. Am. Spine Soc. J.* **8**, 100084. <https://doi.org/10.1016/j.xnsj.2021.100084> (2021).
- Peh, S. et al. Accuracy of augmented reality surgical navigation for minimally invasive pedicle screw insertion in the thoracic and lumbar spine with a new tracking device. *Spine J.* **20**(4), 629–637. <https://doi.org/10.1016/j.spinee.2019.12.009> (2020).
- Elmi-Terander, A. et al. Pedicle screw placement using augmented reality surgical navigation with intraoperative 3D imaging: a first In-Human prospective cohort study. *Spine (Phila Pa. 1976)* **44**(7), 517–525. <https://doi.org/10.1097/brs.0000000000002876> (2019).
- Liu, A. et al. Clinical accuracy and initial experience with augmented reality-assisted pedicle screw placement: the first 205 screws. *J. Neurosurg. Spine* **36**(3), 351–357. <https://doi.org/10.3171/2021.2.spine202097> (2021).
- Yahanda, A. T. et al. First in-human report of the clinical accuracy of thoracolumbar percutaneous pedicle screw placement using augmented reality guidance. *Neurosurg. Focus* **51**(2), E10. <https://doi.org/10.3171/2021.5.focus21217> (2021).
- Yanni, D. S. et al. Real-time navigation guidance with intraoperative CT imaging for pedicle screw placement using an augmented reality head-mounted display: a proof-of-concept study. *Neurosurg. Focus* **51**(2), E11. <https://doi.org/10.3171/2021.5.focus21209> (2021).
- Siemionow, K. B., Katchko, K. M., Lewicki, P. & Luciano, C. J. Augmented reality and artificial intelligence-assisted surgical navigation: technique and cadaveric feasibility study. *J. Craniovertebr Junction Spine* **11**(2), 81–85. https://doi.org/10.4103/jcvjs.JC_VJS_48_20 (2020).
- Kleck, C. J. et al. One-step minimally invasive pedicle screw instrumentation using O-Arm and stealth navigation. *Clin. Spine Surg.* **31**(5), 197–202. <https://doi.org/10.1097/bsd.0000000000000616> (2018).
- Caprara, S. et al. Bone density optimized pedicle screw instrumentation improves screw pull-out force in lumbar vertebrae. *Comput. Methods Biomech. Biomed. Eng.* **25**(4), 464–474. <https://doi.org/10.1080/10255842.2021.1959558> (2022).
- Tuszynski, J. & in_polyhedron. *MATLAB Central File Exchange* (2023, accessed 22 Feb 2023). https://www.mathworks.com/matlabcentral/fileexchange/48041-in_polyhedron.
- Gertzbein, S. D. & Robbins, S. E. Accuracy of pedicular screw placement in vivo. *Spine (Phila Pa 1976)* **15**(1), 11–14. <https://doi.org/10.1097/00007632-199001000-00004> (1990).
- Belmont, P. J. Jr., Klemme, W. R., Robinson, M. & Polly, D. W. Jr. Accuracy of thoracic pedicle screws in patients with and without coronal plane spinal deformities. *Spine (Phila Pa 1976)* **27**(14), 1558–1566. <https://doi.org/10.1097/00007632-200207150-00015> (2002).
- Castro, W. H. et al. Accuracy of pedicle screw placement in lumbar vertebrae. *Spine (Phila Pa 1976)* **21**(11), 1320–1324. <https://doi.org/10.1097/00007632-199606010-00008> (1996).
- Amaral, R., Pimenta, L., Netto, A. G., Pokorny, G. H. & Fernandes, R. Pedicle screws and facet violation—the importance of the angle between the facet and the screw. *Rev. Bras. Ortop. (Sao Paulo)* **55**(5), 642–648. <https://doi.org/10.1055/s-0040-1709200> (2020).
- Matsukawa, K. et al. Incidence and risk factors of adjacent cranial facet joint violation following pedicle screw insertion using cortical bone trajectory technique. *Spine* **41**(14), E851–E866. <https://doi.org/10.1097/BRSS.0000000000001459> (2016).
- Saraf, S. K., Singh, R. P., Singh, V. & Varma, A. Pullout strength of misplaced pedicle screws in the thoracic and lumbar vertebrae—a cadaveric study. *Indian J. Orthop.* **47**(3), 238–243. <https://doi.org/10.4103/0019-5413.111502> (2013).
- Korkmaz, M. et al. Quantitative comparison of a laterally misplaced pedicle screw with a re-directed screw. How much pull-out strength is lost? *Acta Orthop. Traumatol. Turc.* **52**(6), 459–463. <https://doi.org/10.1016/j.aott.2018.03.002> (2018).
- Molina, C. A. et al. A cadaveric precision and accuracy analysis of augmented reality-mediated percutaneous pedicle implant insertion. *J. Neurosurg. Spine* **34**(2), 316–324. <https://doi.org/10.3171/2020.6.spine20370> (2020).
- Frisk, H. et al. Feasibility and accuracy of thoracolumbar pedicle screw placement using an augmented reality head mounted device. *Sens. (Basel)* **22**(2), 522. <https://doi.org/10.3390/s22020522> (2022).

Acknowledgements

We thank PD Dr. med. Michael Betz, Dr. med. Florian Wanivenhaus and Dr. Alexander Spiessberger, for their contribution as investigators in the phantom-based evaluation.

Author contributions

Conceptualization, D.S., C.J.L., F.L., M.F. and P.F.; methodology, D.S., M.F., C.J.L., L.L., J.M.S., P.F., F.C. and F.L.; investigation, D.S., M.F., A.M., L.L. and C.J.L.; resources, M.F. and P.F.; writing—original draft preparation, D.S.; writing—review and editing, M.F., P.F., F.C., C.J.L., A.M. and L.L.; visualization, D.S., A.M. and L.L.; supervision, M.F., P.F., F.C., J.M.S. and C.J.L.; project administration, D.S., C.J.L. and F.C.; funding acquisition, M.F. and P.F. All authors have read and agreed to the published version of the manuscript.

Funding

This research received no external funding.

Competing interests

The authors declare no competing interests.

Additional information

Correspondence and requests for materials should be addressed to D.S.

Reprints and permissions information is available at www.nature.com/reprints.

Publisher's note Springer Nature remains neutral with regard to jurisdictional claims in published maps and institutional affiliations.

Open Access This article is licensed under a Creative Commons Attribution-NonCommercial-NoDerivatives 4.0 International License, which permits any non-commercial use, sharing, distribution and reproduction in any medium or format, as long as you give appropriate credit to the original author(s) and the source, provide a link to the Creative Commons licence, and indicate if you modified the licensed material. You do not have permission under this licence to share adapted material derived from this article or parts of it. The images or other third party material in this article are included in the article's Creative Commons licence, unless indicated otherwise in a credit line to the material. If material is not included in the article's Creative Commons licence and your intended use is not permitted by statutory regulation or exceeds the permitted use, you will need to obtain permission directly from the copyright holder. To view a copy of this licence, visit <http://creativecommons.org/licenses/by-nc-nd/4.0/>.

© The Author(s) 2025